HHS Public Access

Author manuscript

Environ Earth Sci. Author manuscript; available in PMC 2017 June 15.

Published in final edited form as:

Environ Earth Sci. 2017 March ; 76(5): . doi:10.1007/s12665-017-6505-0.

Cross-formational flow of water into coalbed methane reservoirs: controls on relative permeability curve shape and production profile

Alireza Salmachi[1] and **C. Özgen Karacan**[2]

[1]Australian School of Petroleum, University of Adelaide, Adelaide, Australia

[2]Office of Mine Safety and Health Research, NIOSH, Pittsburgh, PA, USA

Abstract

Coalbed methane (CBM) wells tend to produce large volumes of water, especially when there is hydraulic connectivity between coalbed and nearby formations. Cross-formational flow between producing coal and adjacent formations can have significant production and environmental implications, affecting economic viability of production from these shallow reservoirs. Such flows can also affect how much gas can be removed from a coalbed prior to mining and thus can have implications for methane control in mining as well. The aim of this paper is to investigate the impact of water flow from an external source into coalbed on production performance and also on reservoir variables including cleat porosity and relative permeability curves derived from production data analysis. A reservoir model is constructed to investigate the production performance of a CBM well when cross-formational flow is present between the coalbed and the overlying formation. Results show that cleat porosity calculated by analysis of production data can be more than one order of magnitude higher than actual cleat porosity. Due to hydraulic connectivity, water saturation within coalbed does not considerably change for a period of time, and hence, the peak of gas production is delayed. Upon depletion of the overlying formation, water saturation in coalbed quickly decreases. Rapid decline of water saturation in the coalbed corresponds to a sharp increase in gas production. As an important consequence, when cross-flow is present, gas and water relative permeability curves, derived from simulated production data, have distinctive features compared to the initial relative permeability curves. In the case of cross-flow, signatures of relative permeability curves are concave downward and low gas permeability for a range of water saturation, followed by rapid increase afterward for water and gas, respectively. The results and analyses presented in this work can help to assess the impact of cross-formational flow on reservoir variables derived from production data analysis and can also contribute to identifying hydraulic connectivity between coalbed and adjacent formations.

Keywords

Coalbed methane; Cross-formational flow; Reservoir simulation; Relative permeability curve shape; Production data analysis

Correspondence to: Alireza Salmachi.

Introduction

Coalbed degasification is an important practice for minable coalbeds for its effectiveness in improving the safety of underground coal mines and also for the potential of utilizing produced methane as an unconventional energy resource, as well as for reducing greenhouse gas emissions (Karacan et al. 2011; Moore 2012). Coalbed gas drainage activities that were initially undertaken, at least in the USA, for primarily improving mining safety, have improved especially after the development of predictive methods and new drilling and production technologies. This is especially true for the development of coalbed gas reservoir models that are validated using history matching of production wells, which help researchers to gain confidence in the values of assigned coal properties and their distribution within the reservoir. However, coalbeds and their depositional environments are generally more complicated compared to conventional oil or gas reservoirs, and thus production of fluid may not necessarily be confined to the coalbed itself—i.e., there may be cross-flow between coalbed and the overlying formations for different reasons, such as faults, unconformities, and hydraulically induced fractures. Such cross-flows, if not noticed, can result in loss of degasification efficiency, as water will be produced for extended periods of time and also will affect the reservoir variables estimated by history matching methods.

Groundwater hydrology plays an important role in production performance and economics of coalbed methane reservoirs (Pashin 1991; Kaiser 1993; Ayers and Kaiser 1994; Scott 2002). Water production from coalbeds has environmental and economic implications for CBM development projects, depending on the volume of water produced and cost of water treatment and disposal. The average water production rate for CBM wells in eastern Australia is about 188 STB per day, and it can vary from only a few barrels per day per well up to thousands of barrels per day per well across a reservoir (CISERA 2014). Salmachi et al. (2013, 2014) have discussed the impact of water production and cost of treatment and disposal for well placement in developed coalbed methane reservoirs.

Groundwater hydrology in a coalbed methane reservoir is controlled by the geology of the area. Confinement by impermeable formations, faults, presence of outcrops, and unconformity are some of the geological factors that may affect coal hydrology. Hydrodynamics of coalbed methane reservoirs of Black Warrior Basin (western Alabama, USA), San Juan Basin (encompassing parts of New Mexico, Colorado, Arizona, and Utah, USA), Uinta and Piceance Basins (Utah, USA), and Colorado River Basin (USA) have been investigated in the context of the geological setting (Anna 2003; Pashin 2007; Council 2010). Thick impermeable marine shales in the Black Warrior Basin limit cross-communication of fluids and restrict the flow into coal zones (Pashin 2007). Faults, regardless of their types, can affect fluid flow within coal zones (Moore 2012). The effect of faults on gas and water production has been investigated in Deerlick Creek, Cedar Cove, and Oak Grove fields in the Black Warrior Basin (western Alabama, USA), and also the Roma gas field in the Surat Basin in Australia (Sparks et al. 1993; Pashin 1998; Santos-GLNG 2014). Impermeable faults can result in reservoir compartmentalization and reduce degasifying efficiency, especially in vertical wells (Karacan et al. 2008). On the other hand, permeable faults that lie within a production area may provide viable avenues for hydraulic communication with nearby formations.

Permeability is also an important controlling factor in hydrology of coalbeds. Holditch (1993) suggested that coal permeability in the range of 1–100 mD is optimum to achieve economical gas flowrate. Ultra-high permeable coals might be difficult to dewater, especially when cross-formational flow exists. The other geological factor that may establish hydraulic connectivity between nearby formations and the coalbed is the unconformity. Unconformity can remove formations that are effective seals for a reservoir and create a contact zone between the coal and an overlying aquifer. The Precipice contact zone in the Fairview Field has been studied to investigate the hydraulic connectivity between the Bandanna Formation (target formation in the Fairview field) and the Precipice sandstone. At the Precipice contact zone, the Rewan Formation generally isolating the Bandanna Formation is absent (Santos-GLNG 2014).

Figure 1 is a conceptual model illustrating potential cross-flow scenarios established artificially by wellbore stimulation or present naturally due to geological setting of the area. Propagation of complex hydraulic fractures into nearby formations increases the chance of cross-flow. It was found that hydraulically stimulated fractures in coalbeds of the Powder River Basin could potentially extend into neighboring formations and result in excessive water production and inefficient reservoir depletion (Colmenares and Zoback 2007). The occurrence of cross-formational flow in a contact zone is also conceptually illustrated in Fig. 1. High permeable coal in a contact zone is an ideal avenue to discharge water from nearby formations.

In the case of cross-formational flow, reservoir parameters obtained by production data analysis techniques can be affected. Production data analysis is a powerful tool assisting researchers in attaining some significant reservoir properties as well as stimulation parameters. Recent advances in production data and rate transient analyses help researchers to obtain vital CBM reservoir properties such as permeability-thickness product (Kh), skin factor, initial gas and water in place, and time of peak gas production (Mohaghegh and Ertekin 1991; Aminian et al. 2004; Clarkson et al. 2012; Clarkson 2013; Karacan 2013; Salmachi and Yarmohammadtooski 2015). Production data analysis in CBM reservoirs can be complicated due to factors such as adsorption-driven gas storage mechanism, difficulties in determining relative permeability, and stress/desorption-dependent permeability (Clarkson et al. 2007a).

One of complexities affecting PDA is relative permeability. Characteristics of relative permeability curves determine fluid production (Chen et al. 2013) and are essential for field and simulation studies (Shi et al. 2008; Clarkson et al. 2011). Relative permeability curves are generally shown as a function of wetting phase saturation. Relative permeability of coals has been measured in the laboratory by various authors (Dabbous et al. 1974; Reznik et al. 1974; Gash 1991; Purl et al. 1991; Hyman et al. 1992; Meaney and Paterson 1996; Shi et al. 2008; Shen et al. 2011). For CBM wells drilled in water-saturated coals, gas and water relative permeability curves can be derived from field data as the depletion progresses. The more the coal is dewatered, the larger the water saturation range is available to derive relative permeability curves (Seidle 2011). Clarkson et al. (2011) introduced a workflow to generate relative permeability curves from actual production data. However, relative permeability curves obtained by production history matching are generally different from

laboratory measured curves due to viscous fingering and buoyancy effects, which are incorporated into history matched derived curves but not in the ones measured in the laboratory (Seidle 2011).

This study aims to investigate cross-formational flow between producing coalbed and adjacent formations in a contact zone by reservoir simulation. For this purpose, a simulation model is constructed and cross-flow is allowed between the coalbed and the overlying formation. The generated production data are interpreted to demonstrate the effect of cross-flow on production performance of the well. Cleat porosity and relative permeability curves are derived from simulated production data to indicate the difference between derived and actual reservoir variables and to highlight the impact of cross-formational flow on production data analysis.

Methodology

In the present work, a simulation study is performed to generate gas and water production data while cross-formational flow is present between the coalbed and the overlying formation. Cleat porosity is calculated by water production data, and a tank-type model is used to derive relative permeability curves from simulated 2-phase flow production data. It should be noted that we intentionally violate the assumption of no-flow boundary by applying the tank-type model. This is equivalent to using the tank-type model to extract reservoir engineering parameters while cross-formational flow is not detected. This study demonstrates how reservoir parameters obtained by production data analysis may be affected by cross-flow. The workflow in Fig. 2 shows the steps and methods used to derive cleat porosity and relative permeability curves from simulated production history.

Simulation model

A single-well simulation model is constructed using the Computer Modelling Group (CMG) reservoir simulator. We try to keep the simulation model as simple as possible to exclusively study the cross-formational flow effect. Although this model does not replicate a particular well, most of the input variables have been selected based on the USA and the Australian CBM reservoir properties. Table 1 shows the input variables used in the simulation model.

The following models and assumptions are used in the model to simulate gas and water flow in the coalbed:

1. Dual porosity.
2. Non-equilibrium sorption.
3. Palmer–Mansoori rock type compaction.
4. Langmuir-type sorption isotherm.
5. Single component gas (methane).
6. Isothermal reservoir condition.

In dual porosity model, fracture and matrix are modeled as two separate grid blocks, thus allowing one porosity for fracture and one porosity for matrix in each grid block. The

amount of gas stored in the adsorbed phase at any pressure is described by the Langmuir isotherm and is in equilibrium with the matrix pressure. Dewatering reduces the pressure in the cleat system down to the critical desorption pressure at which gas starts desorbing and diffusing in coal matrix. Non-equilibrium sorption model describes the total mass transfer rate from coal matrix to cleat network by the product of a diffusion coefficient and a matrix shape factor. This product is known as the sorption time which is widely used in coalbed methane reservoir simulators (MacLennan et al. 1995). Gas and water relative permeability curves are used to explain relative flow of gas and water in the cleat system.

Figure 3 shows the plan and 3D views of the simulation model. The coalbed is confined between an overlying high permeable formation and an impermeable formation at the base. Coalbed permeability is set to 217 mD, which puts the reservoir in the category of ultra-high permeable coals (Palmer 2010), and this may simulate the condition where coal is situated in the fairway of a field. The reservoir is normally pressured and has an initial pressure of 942 psia at the reservoir depth of 2194 ft. The initial gas content of 430 SCF/ton results in the critical desorption pressure of 837 psia. Hence, dewatering is required prior to commencing gas production. The overlying formation is saturated with water and is hydraulically connected to the coalbed. Hydraulic connectivity can be established through vertical permeability of the coalbed and the overlying formation. This simulates the condition where the producing coalbed is located in a contact zone and water can freely flow from the overlying formation into the producing coalbed. Note that hydraulic connectivity can also exist due to vertical fractures or permeable faults extending from coal into surrounding formations.

Gas and water relative permeability curves, shown in Fig. 4, are assigned to the coalbed and the overlying formation to generate gas and water production data. The wellbore is completed and perforated within the coal zone. Hence, fluid flow into the wellbore is only restricted into the coal interval. Two operational constraints are defined for the wellbore—a maximum surface water rate of 4000 STB/day and the minimum bottom-hole pressure of 200 psia. Reservoir simulation is performed for about 22 years (equivalent to 8000 days) to simulate gas and water flow in the coalbed and the overlying formation. The water storage capacity of the overlying formation is adjusted by changing the porosity to create two simulation cases. In both cases, the level of hydraulic connectivity (permeability) is the same; however, in the first case, a larger volume of water flows to the producing coalbed compared to the second case. Permeability enhancement and vertical conductivity effects on cross-formational flow are studied in the third and fourth cases, respectively.

Production data analysis

The tank-type model is a popular method to study the depletion of gas and water in a bounded CBM well (Seidle 2011). It can be used to construct relative permeability curves using field/simulated production data. The five-step workflow, introduced by Clarkson et al. (2011), is employed to generate gas and water relative permeability curves. Material balance equations (Eqs. 1–3) for coalbeds (King 1993) are used to calculate average reservoir pressure and water saturation. In this study, pressure-squared formulation (Eq. 4) is used to

calculate gas relative permeability. Water relative permeability is calculated by a pseudo-steady-state equation (Eq. 5).

$$S_{\mathrm{w}}=S_{\mathrm{wi}}-\frac{B_{\mathrm{w}}}{7758.4Ah\varnothing}W_{\mathrm{p}} \quad (1)$$

$$\frac{p}{Z^*}=\frac{p_{\mathrm{i}}}{Z_{\mathrm{i}}^*}\left(1-\frac{G_{\mathrm{p}}}{G_{\mathrm{i}}}\right) \quad (2)$$

$$Z^*=\frac{Z}{\frac{\rho_{\mathrm{B}}V_{\mathrm{Ldaf}}(1-a-w)P_{\mathrm{sc}}TZ}{32.037\varnothing Z_{\mathrm{sc}}T_{\mathrm{sc}}(p+p_{\mathrm{L}})}+(1-S_{\mathrm{w}})} \quad (3)$$

$$K_{\mathrm{rg}}=\frac{q_{\mathrm{g}}\left[1422T\,\overline{Z\mu_{\mathrm{g}}}\left(\ln\left(\frac{r_{\mathrm{e}}}{r_{\mathrm{w}}}\right)-0.75+s\right)\right]}{K_{\mathrm{abs}}h\left(P_{\mathrm{R}}^2-P_{\mathrm{wf}}^2\right)} \quad (4)$$

$$k_{\mathrm{rw}}=\frac{q_{\mathrm{w}}\left[141.2B_{\mathrm{w}}\mu_{\mathrm{w}}\left(\ln\left(\frac{r_{\mathrm{e}}}{r_{\mathrm{w}}}\right)-0.75+s\right)\right]}{K_{\mathrm{abs}}h(P_{\mathrm{R}}-P_{\mathrm{wf}})} \quad (5)$$

Discussion and analysis

Four simulation cases are presented to investigate the impact of cross-formational flow on production performance of CBM wells. In all cases, the contact zone is extended all over the drainage area feeding the coalbed with water during production period. In the first case, the water storage capacity of the overlying formation is high (high porosity) allowing substantial amount of water flows into the coalbed during production. In the second case, the water storage capacity of the overlying formation is reduced (lower porosity) while the rest of the parameters are similar to the first case. In the third case, cross-formational flow and permeability enhancement occur simultaneously, and hence, the role of permeability variation on cross-flow can be studied. In the fourth case, the impact of vertical conductivity between coalbed and the overlying formation on cross-flow is studied by adjusting the vertical permeability of the overlying formation.

Case 1

Gas and water production data are generated by the reservoir simulator for this case when absolute permeability of the coalbed is constant. Figure 5a shows the simulated gas and water production history for the well. The production profile is separated into an early

production period (single-phase water flow) and two-phase (gas and water) flow period. At the early production period, single-phase flow of water is observed (gas production is negligible) for about 1 year prior to the two-phase flow of gas and water. The water production rate rapidly increases and stabilizes at 4000 STB/day which is the production constraint specified in the simulation model. There are two distinctive decline shapes on the water production profile, indicating that water is depleted from two different sources—the overlying formation and the coal section. Average water saturation within the coal and the overlying formation is shown in Fig. 5b. Although considerable volume of water is produced from the well, average water saturation in coal is approximately constant for 8 years. This is due to water discharge from the overlying formation replacing the produced water from the coal section. While average water saturation in coal remains close to 1 for an extended period of time, average water saturation in the overlying formation sharply decreases. Cross-flow of water between the coal and the adjacent formation significantly reduces the efficiency of the dewatering operation, and consequently gas production is hindered.

Initially, high water saturation in coalbed results in very low gas relative permeability, and consequently, gas production rates are very low. Upon depletion of the overlying formation, average water saturation in coal declines (see Fig. 5b). Decline in water saturation in coal corresponds to a sharp increase in gas production rate which exceeds 2 MMSCF/day at the peak of production and then exponentially declines (see Fig. 5a). Rapid increase in gas production may serve as a signature showing that cross-formational flow diminishes.

Desorbed gas partly migrates to the overlying formation and replaces the water. Hence, the overlying formation acts as a thief zone accommodating desorbed gas from the coal matrix. Figure 6 shows the evolution of gas saturation in the overlying formation for the first 6 years of production. Hydraulic connectivity among the coalbed and the overlying formation allows fluid flow to occur in both directions. Water flows toward the coal section and desorbed gas replaces the produced water, and eventually, the top formation is depleted from the water and is saturated with gas. Gas migration to the overlying formation may affect the production performance and have environmental implications. In this example, the impact of the thief zone on production profile is negligible due to the low pressure and storage capacity of the overlying formation. Environmental implications of gas migration to adjacent formations are more important because fresh water aquifers may be contaminated if the contact zone is extended to nearby aquifers. Hence, it is vital to conduct hydraulic connectivity assessment in coalbed methane reservoirs when cross-flow is suspected.

Cleat porosity, calculated by production history matching techniques, is very sensitive to water production data. Table 2 shows the cleat porosities either used in or derived from matching techniques in various basins worldwide. The cleat porosity derived from matching techniques varies from 0.035 up to 6% in the literature. The variability in cleat porosity is attributed to the water production data which is used to calculate cleat porosity in matching techniques. In our study, simulated water production data include both the volume of the water produced from the coalbed and the volume of the water produced from the overlying formation. Hence, cleat porosity calculation is highly affected when the volume of the water flowing from the overlying formation is not excluded from the production data. Cleat porosity of 3.7% is obtained when cumulative water production data are used, which is 18.5

times higher than the actual cleat porosity of 0.2% used in the simulation model. Cross-formational flow is responsible for higher than actual cleat porosity obtained by the analysis of production data.

The results of this simulation study are in agreement with the study conducted by Palmer et al. (2011) on cleat porosity measurement in coals. Production data analysis of CBM wells with relatively high water production rates leads to cleat porosities up to 3–5%. An example is the north of fairway in the San Juan Basin in the USA, where CBM wells produce water over 1000 STB/day. The large volume of water produced from the wells is probably extracted from an external source (Palmer et al. 2011).

Relative permeability curve shape greatly varies in CBM reservoirs (Zuber et al. 1987; Clarkson et al. 2011; Seidle 2011) and can be influenced by net stress, porosity change, and viscous fingering and buoyancy effects (Reznik et al. 1974; Clarkson et al. 2007b; Seidle 2011; Chen et al. 2013). In this study, relative permeability curves are derived from simulated 2-phase flow production data by the workflow presented in Fig. 2. Derived gas and water relative permeability curves are compared with input curves in Fig. 5c, and clearly the impact of cross-flow can be observed on the derived curves. The discrepancy between input and derived relative permeability curves is due to the calculation of wetting phase saturation by cumulative water production, which includes volume of produced water from both coal and overlying formations. When cross-formational flow is not detected, derived relative permeability curves are affected and have irregular shapes. Water relative permeability curve is concave downward due to the excessive volume of water produced from the overlying formation. Gas relative permeability is initially very low and changes slightly, then at the average water saturation of about 40% it rises.

Results indicate that when hydraulic communication between the producing coalbed and the adjacent formation is not detected, reservoir variables including cleat porosity and relative permeability curves derived from PDA are not reliable. Note that in this case, due to a large volume of water flowing from the overlying formation, the signature of cross-flow is readily identified on reservoir variables including cleat porosity and relative permeability curves. The degree of influence of cross-flow on derived reservoir parameters depends on the volume of water flowing from the external source. The cross-flow effect on the production profile is lessened when a low volume of water is discharged from the adjacent formation into the coal section. Low-intensity cross-flow and its associated effects on production performance and production data analysis are discussed in the next example.

Case 2

In this example, the porosity of the overlying formation is reduced from 9.16% (in the first case) down to 2% and, as a result, the water storage capacity of the overlying formation is reduced. This decreases the contribution of the overlying formation to total water production, and consequently the impact of cross-formational flow is alleviated. Gas and water production data for this case are presented in Fig. 7a.

The shape of the water production profile resembles production data of a bounded well drilled in an under-saturated CBM reservoir. Hence, the signature of cross-flow on the water

production profile is not evident. Water saturation within the coalbed reduces more quickly compared to the first case (see Fig. 7b), and as a result, gas mobility increases. Time of peak gas production is brought forward, and gas production rate reaches to 3.6 MMSCF/day at the peak of production. Cumulative gas production of 10.76 BCF results in total gas recovery of 41.8%. This is higher than gas recovery factor of 29.6% calculated for the first case. Higher recovery factor is attained because gas saturation and relative permeability evolve more quickly.

When cross-formational flow is ignored, cleat porosity of 0.87% is calculated by the analysis of cumulative water production data. Note that cleat porosity of 0.87% which is 4 times higher than actual porosity used in the simulation maybe incorrectly considered as an acceptable value for reservoir engineering purposes. Although cross-formational flow exists, its effect on cleat porosity is likely to be unnoticed due to lower volume of water flowing from the external source. Gas and water relative permeability curves derived from production data are shown in Fig. 7c and are compared with the input curves. The effect of cross-flow on derived relative permeability curves is moderated when compared with the first case in which significant volume of water is produced from the external source. Cross-flow imposes two important features on relative permeability curves shown in Fig. 7c. First, the water relative permeability curve is close to a straight line. Second, critical gas saturation is high for the gas relative permeability curve. Note that these features are related to cross-flow effect and do not represent fluid flow characteristics of the coal formation.

The shapes of relative permeability curves in Fig. 7c are similar to some of the coal relative permeability curves investigated in the literature (Purl et al. 1991; Shi and Durucan 2004; Clarkson et al. 2011; Chen et al. 2013). Hence, the signature of cross-flow on derived relative permeability curves may be ignored due to this similarity. It is important to investigate the groundwater hydrology of the area when derived relative permeability curve shapes are similar to those demonstrated in this study.

Case 3

In this example, cross-formational flow and permeability enhancement are simultaneously occurred. Reservoir properties are similar to those used in the first case except for coal permeability which is pressure and desorption-dependent. Palmer–Mansoori model is used to incorporate the effect of compaction and matrix shrinkage into coal permeability, and the parameters used in the permeability model are listed in Table 3.

Figure 8a compares gas and water production history of this example in which coal permeability is dynamic and sensitive to pore pressure and matrix shrinkage with the first case when coal permeability is constant. Due to strong shrinkage, coal permeability starts to rise shortly after production commences, and hence, water depletion is facilitated and water is produced at a constant rate of 4000 STB/day for approximately 3 years before it starts to decline. Initially, water production profile is concave downward indicating the impact of permeability increase on water production rates. Average water saturation in the overlying formation, shown in Fig. 8b, declines more rapidly compared to the first case, indicating that permeability enhancement facilitates water depletion in both overlying and coal formations. Figure 8c shows horizontal coal permeability variation with time which is due to

simultaneous actions of two opposing factors on coal permeability—matrix shrinkage and cleat compaction. Note that coal permeability increases in both horizontal and vertical directions and thus hydraulic connectivity with the overlying formation is improved during production.

Both peak of gas production and time to reach to peak of production are affected by permeability enhancement. Peak of gas production is about 4 MMSCF/day which is double that of the first case, and time to reach to peak of gas production is brought forward to 3200 days. Permeability enhancement facilitates gas and water production from coalbed and the overlying formation which are opposing factors in economics of CBM wells.

Case 4

Vertical conductivity between producing coalbed and overlying aquifers can be promoted by existence of major faults, complex fault systems, or coal fractures extending into nearby formations. The existence of complex fault system and major fractures extending from coalbed into overburden layers may be identified by borehole image logs (Reynolds et al. 2003; Rajabi et al. 2016a, b). This case demonstrates how vertical conductivity established between coalbed and the overlying formation affects production profile. Vertical permeability of the overlying formation is set to 1 mD in the simulation model to establish a lower level of connectivity between coalbed and the overlying formation compared to the first case. In this case, cross-formational flow is restricted by vertical permeability of the overlying formation (1 mD) which is lower than vertical permeability of the coalbed (21.7 mD). Figure 9 compares production profile and water saturation change in coal and overlying formations of this case with the ones in the first case.

Due to restricted cross-formational flow, imposed by vertical permeability of the overlying formation, water flows from the overlying formation into coalbed at lower rates compared to the first case. Water continuously leaks to the coal over the life of the well, and hence, water saturation in coal remains high. After about 5000 days, water saturation starts to stabilize at about 60% and rebounds very slightly afterward (see Fig. 9). Water saturation stabilization in coal at 60% is because of water rate into coalbed becomes equal to water production rate. Later, water rate from the overlying formation slightly exceeds the water production rate, and hence, water saturation rebounds very slightly. When relative permeability curves are derived from production data (see Fig. 10), signature of cross-formational flow can be observed on the curves. Water saturation stabilization/rebound in coal results in derived relative permeability curve shapes to be approximately flat when calculated water saturation is between 0.2 and 0.1. Note that the calculated water saturation is based on the assumption that cross-flow does not exist; hence, it is different from actual water saturation shown in Fig. 9 for coal and the overlying formation.

Conclusion

Simulation results indicate that CBM wells located in a contact zone produce large volumes of water, and production rate depends on the level of connectivity established between the producing coalbed and nearby formations. Cross-flow of water tends to keep water saturation high within the coalbed for a period of time, and consequently the peak of gas

production is postponed. Once the adjacent formation, which is hydraulically connected to the coalbed, is sufficiently depleted from water, water saturation in coal declines. The decline in coal water saturation corresponds to rapid increase in gas production. This quick increase in gas production is a feature in the production profile that might be served as a signature, indicating that cross-formational flow diminishes.

Cross-formational flow of water from an external source into the producing coalbed affects calculations performed by production data and also interpretations related to reservoir parameters and dynamics. When cross-formational flow is not detected, cleat porosity calculated by cumulative water production data is higher than actual cleat porosity. Gas and water relative permeability curves constructed by simulated production data are also different than the initial relative permeability curves and have distinctive features. Water relative permeability is high, and the curve could be even concave downward. Higher than expected, water relative permeability is due to the excess water flowing from the external source into the producing coal. Gas relative permeability is very low for a range of water saturation and then sharply rises. Although relative permeability curves are often used as history matching parameters, the assumption that the entire flow being from the coalbed may still lead to erroneous relative permeability curves, even after history matching. Therefore, hydraulic connectivity assessment should be performed to confirm the hydraulic communication and its intensity within the area using well logs or zone isolation tests, when the cross-flow is suspected. This helps to mitigate environmental problems associated with cross-flow effects and maximizes production efficiency for future field development plans.

Acknowledgments

We would like to acknowledge Dr Ian Palmer for providing extremely useful and constructive comments on this paper. We also like to thank the anonymous reviewers for their time and comments that helped us to improve the quality of this research paper.

List of symbols

A	Area (acres)
a	Ash content (fraction)
B_w	Water formation volume factor (rb/stb)
G_i	Initial gas in place (scf)
G_p	Cumulative gas production (scf)
h	Coal thickness (ft)
K_{abs}	Absolute permeability (mD)
K_{rg}	Gas relative permeability
K_{rw}	Water relative permeability
m	Moisture content (fraction)

p_i	Initial pressure (psia)
p_L	Langmuir pressure (psia)
P_{wf}	Flowing bottom-hole pressure (psia)
P_R	Reservoir pressure (psia)
q_g	Gas flowrate (mscf/day)
q_w	Water flowrate (STB/day)
r_e	External radius (ft)
r_w	Wellbore radius (ft)
s	Skin factor
S_w	Water saturation
S_{wi}	Initial water saturation
T	Temperature (Rankin°)
T_{sc}	Temperature at standard condition (Rankin°)
V_{Ldaf}	Langmuir volume (dry-ash free, scf/ton)
W_p	Cumulative water production (STB)
Z	Gas compressibility factor
μ_g	Gas viscosity (cP)
μ_w	Water viscosity (cP)
$Ø$	Porosity (fraction)
ρ_B	Bulk coal density (g/cm^3)

References

Aminian, K., Ameri, S., Bhavsar, A., Sanchez, M., Garcia, A. Type curves for coalbed methane production prediction. SPE eastern regional meeting. Society of Petroleum Engineers; Charleston, WV. 2004. SPE-91482

Anna L. Groundwater flow associated with coalbed gas production, Ferron Sandstone, east-central Utah. Int J Coal Geol. 2003; 56(1–2):69–95.

Ayers W Jr, Kaiser W. Coalbed methane in the upper cretaceous fruitland formation. San Juan Basin, Colorado and New Mexico. Texas Bureau Econ Geol Rep Investig. 1994; 218:216.

Chen D, Pan Z, Liu J, Connell L. An improved relative permeability model for coal reservoirs. Int J Coal Geol. 2013; 109:45–57.

CISERA. Coal seam gas-produced water and site management. Gas Industry Social & Environmental Research Alliance. 2014. http://www.gisera.org.au/publications/scientificreports.html

Clarkson C. Production data analysis of unconventional gas wells: review of theory and best practices. Int J Coal Geol. 2013; 109:101–146.

Clarkson, C., Jordan, C., Gierhart, R., Seidle, J. Production data analysis of CBM wells. Rocky mountain oil and gas technology symposium; Denver, CO: Society of Petroleum Engineers; 2007a. SPE-107705

Clarkson CR, Bustin RM, Seidle JP. Production-data analysis of single-phase (gas) coalbed-methane wells. SPE Reserv Eval Eng. 2007b; 10(03):312–331.

Clarkson C, Rahmanian M, Kantzas A, Morad K. Relative permeability of CBM reservoirs: controls on curve shape. Int J Coal Geol. 2011; 88(4):204–217.

Clarkson C, Jordan C, Ilk D, Blasingame T. Rate-transient analysis of 2-phase (gas + water) CBM wells. J Nat Gas Sci Eng. 2012; 8:106–120.

Colmenares LB, Zoback MD. Hydraulic fracturing and wellbore completion of coalbed methane wells in the Powder River Basin, Wyoming: implications for water and gas production. AAPG Bull. 2007; 91(1):51–67.

Council NR. Management and effects of coalbed methane produced water in the Western United States, DC. The National Academies Press; Washington: 2010.

Dabbous M, Reznik A, Taber J, Fulton P. The permeability of coal to gas and water. Soc Petrol Eng J. 1974; 14(06):563–572.

Gash, B. Measurement of “rock properties” in coal for coalbed methane production. SPE annual technical conference and exhibition. Society of Petroleum Engineers; Dallas, TX. 1991. SPE-22909

Holditch SA. Completion methods in coal-seam reservoirs. SPE J Petrol Technol. 1993; 45(3):270–276.

Hyman L, Brugler M, Daneshjou D, Ohen H. Advances in laboratory measurement techniques of relative permeability and capillary pressure for coal seams. Q Rev Methane Coal Seams Technol. 1992; 9(2):9–13.

Kaiser, W. Abnormal pressure in coal basins of the western United States. Proceedings of the 1993 international coalbed methane symposium. The University of Alabama, School of Mines and Energy Development; 1993.

Karacan C. Production history matching to determine reservoir properties of important coal groups in the Upper Pottsville formation, Brookwood and Oak Grove fields, Black Warrior Basin, Alabama. J Nat Gas Sci Eng. 2013; 10:51–67. [PubMed: 26191096]

Karacan CÖ, Ulery JP, Goodman GVR. A numerical evaluation on the effects of impermeable faults on degasification efficiency and methane emissions during underground coal mining. Int J Coal Geol. 2008; 75(4):195–203.

Karacan CÖ, Ruiz FA, Cotè M, Phipps S. Coal mine methane: a review of capture and utilization practices with benefits to mining safety and to greenhouse gas reduction. Int J Coal Geol. 2011; 86(2–3):121–156.

Karacan C, Drobniak A, Mastalerz M. Coal bed reservoir simulation with geostatistical property realizations for simultaneous multi-well production history matching: a case study from Illinois Basin, Indiana, USA. Int J Coal Geol. 2014; 131:71–89.

King G. Material-balance techniques for coal-seam and devonian shale gas reservoirs with limited water influx. SPE Reserv Eng. 1993; 8(01):67–72.

MacLennan, J., Schafer, P., Pratt, T. A guide to determining coalbed gas content. Gas Research Institute; Des Plaines: 1995.

Mazumder, S., Jiang, J., Sharma, V., Sugiarto, I. Production data analysis of CBM wells in Surat Basin. SPE unconventional resources conference and exhibition-Asia Pacific. Society of Petroleum Engineers; Brisbane. 2013. SPE 167076

McKee C, Bumb A. Flow-testing coalbed methane production wells in the presence of water and gas. SPE Form Eval. 1987; 2(04):599–608.

Meaney, K., Paterson, L. Relative permeability in coal. SPE Asia pacific oil and gas conference. Society of Petroleum Engineers; Adelaide. 1996. SPE-36986-MS

Mohaghegh, S., Ertekin, T. A type-curve solution for coal seam degasification wells producing under two-phase flow conditions. SPE annual technical conference and exhibition. Society of Petroleum Engineers; Dallas, TX. 1991. SPE-22673

Moore, RL., Loftin, DF., Palmer, ID. History matching and permeability increases of mature coalbed methane wells in San Juan Basin. SPE Asia pacific oil and gas conference and exhibition. Society of Petroleum Engineers; Jakarta, Indonesia. 2011. SPE-146931-MS

Moore T. Coalbed methane: a review. Int J Coal Geol. 2012; 101:36–81.

Palmer I. Coalbed methane completions: a world view. Int J Coal Geol. 2010; 82(3–4):184–195.

Palmer, I., Moore, B., Loftin, D. Cleat porosity of coals: new understanding. Processings Asia-pacific coalbed methane conference; Brisbane: University of Queensland; 2011.

Pashin, J. Regional analysis of the Black Creek-Cobb coalbed-methane target interval. Geological Survey of Alabama, Black Warrior Basin; 1991.

Pashin JC. Stratigraphy and structure of coalbed methane reservoirs in the United States: an overview. Int J Coal Geol. 1998; 35(1):209–240.

Pashin J. Hydrodynamics of coalbed methane reservoirs in the Black Warrior Basin: key to understanding reservoir performance and environmental issues. Appl Geochem. 2007; 22(10): 2257–2272.

Purl, R., Evanoff, J., Brugler, M. Measurement of coal cleat porosity and relative permeability characteristics. SPE gas technology symposium. Society of Petroleum Engineers; Houston, TX. 1991. SPE-21491-MS

Rajabi M, Tingay M, Heidbach O. The present-day state of tectonic stress in the Darling Basin, Australia: implications for exploration and production. Mar Pet Geol. 2016a; 77:776–790.

Rajabi M, Tingay M, Heidbach O. The present-day stress field of New South Wales, Australia. Aust J Earth Sci. 2016b; 63(01):1–21.

Reynolds S, Hillis R, Paraschivoiu E. In situ stress field, fault reactivation and seal integrity in the Bight Basin, South Australia. Explor Geophys. 2003; 34(3):174–181.

Reznik A, Dabbous M, Fulton P, Taber J. Air–water relative permeability studies of Pittsburgh and Pocahontas coals. Soc Pet Eng J. 1974; 14(06):556–562.

Ried, G., Towler, B., Harris, H. Simulation and economics of coalbed methane production in the Powder River Basin. SPE rocky mountain regional meeting. Society of Petroleum Engineers; Casper, WY. 1992. SPE-24360-MS

Salmachi A, Yarmohammadtooski Z. Production data analysis of coalbed methane wells to estimate the time required to reach to peak of gas production. Int J Coal Geol. 2015; 141–142:33–41.

Salmachi A, Sayyafzadeh M, Haghighi M. Infill well placement optimization in coal bed methane reservoirs using genetic algorithm. Fuel. 2013; 111:248–258.

Salmachi A, Bonyadi M, Sayyafzadeh M, Haghighi M. Identification of potential locations for well placement in developed coalbed methane reservoirs. Int J Coal Geol. 2014; 131:250–262.

Santos-GLNG. S. Development. Brisbane: Queensland Government; 2014. Hydraulic connectivity characterisation. http://eisdocs.dsdip.qld.gov.au/Santos%20GLNG%20Gas%20Field%20Development/EIS/Appendices/appendix-ae-a-hydraulic-connectivity-characterisation.pdf

Sawyer, W., Paul, G., Schraufnagel, R. Development and application of a 3-D coalbed simulator. Annual technical meeting. Petroleum Society of Canada; Calgary, AB. 1990. PETSOC-90–119

Scott AR. Hydrogeologic factors affecting gas content distribution in coal beds. Int J Coal Geol. 2002; 50(1):363–387.

Seidle, J. Fundamentals of coalbed methane reservoir engineering. PennWell Books; Tulsa, OK: 2011.

Shen J, Qin Y, Wang G, Fu X, Wei C, Lei B. Relative permeabilities of gas and water for different rank coals. Int J Coal Geol. 2011; 86(2):266–275.

Shi, JQ., Durucan, S. A numerical simulation study of the Allison unit CO_2-ECBM pilot: the impact of matrix shrinkage and swelling on ECBM production and CO_2 injectivity. Proceedings of 7th international conference on greenhouse gas control technologies; 2004.

Shi J-Q, Durucan S. Exponential growth in San Juan Basin Fruitland coalbed permeability with reservoir drawdown: model match and new insights. SPE Reserv Eval Eng. 2010; 13(06):914–925.

Shi J, Durucan S, Fujioka M. A reservoir simulation study of CO_2 injection and N_2 flooding at the Ishikari coalfield CO_2 storage pilot project, Japan. Int J Greenhouse Gas Control. 2008; 2(1):47–57.

Sparks, D., Lambert, S., McLendon, T. Coalbed gas well flow performance controls, Cedar Cove Area, Warrior Basin, USA, Paper 9376. Proceedings of the 1993 international coalbed methane symposium; Tuscaloosa, AL. 1993.

Wong S, Law D, Deng X, Robinson J, Kadatz B, Gunter WD, Jianping Y, Sanli F, Zhiqiang F. Enhanced coalbed methane and CO_2 storage in anthracitic coals—micro-pilot test at South Qinshui, Shanxi, China. Int J Greenhouse Gas Control. 2007; 1(2):215–222.

Yarmohammadtooski Z, Salmachi A, White A, Rajabi M. Fluid flow characteristics of bandanna coal formation: A case study from fairview field, eastern Australia. Aust J Earth Sci. 2016; doi: 10.1080/08120099.2017.1292316

Young, G., McElhiney, J., Paul, G., McBane, R. An analysis of Fruitland coalbed methane production, Cedar Hill field, northern San Juan Basin. SPE annual technical conference and exhibition. Texas Society of Petroleum Engineers; Dallas. 1991.

Zuber, M., Sawyer, W., Schraufnagel, R., Kuuskraa, V. The use of simulation and history matching to determine critical coalbed methane reservoir properties. Low permeability reservoirs symposium. Society of Petroleum Engineers; Denver, CO. 1987.

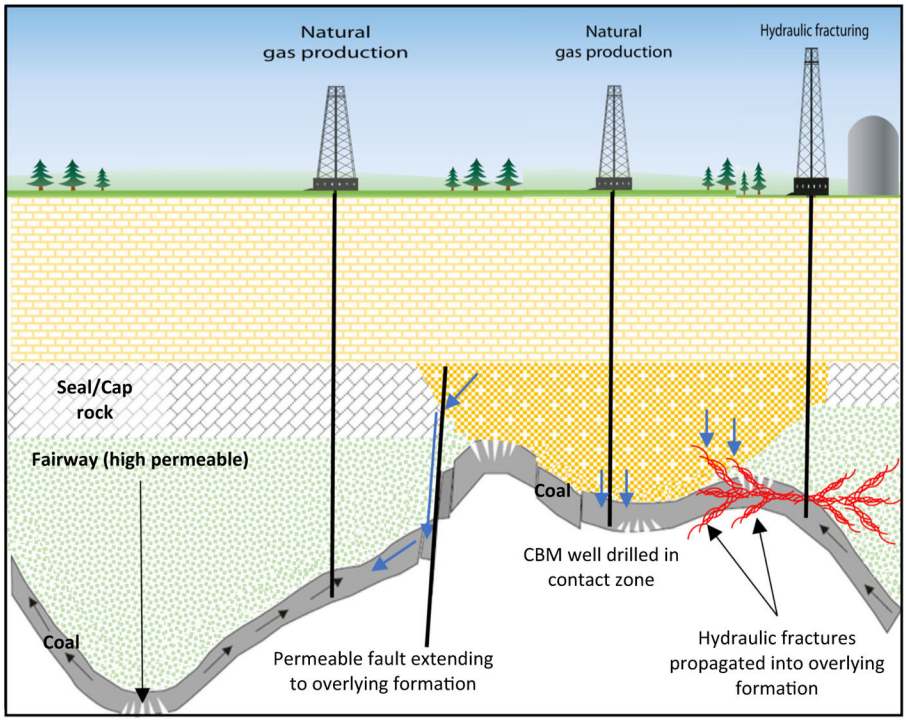

Fig. 1.

Conceptual model illustrating cross-formational flow due to geological factors including permeable faults and contact zone near to producing CBM wells. The figure also shows that cross-flow can be established artificially by propagation of hydraulic fractures into adjacent formations

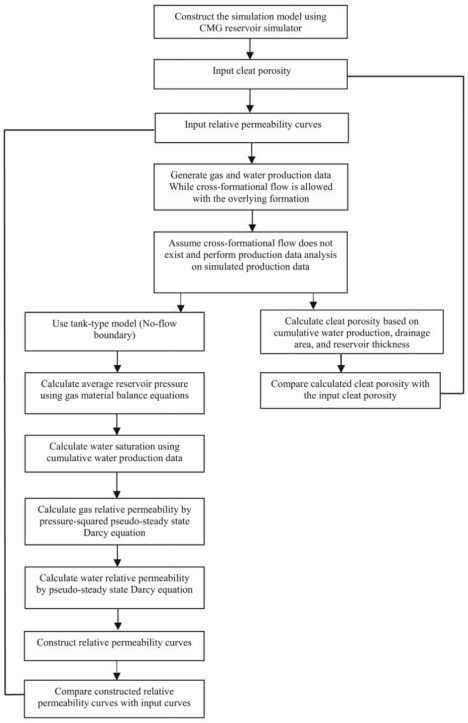

Fig. 2.

Generalized workflow to derive relative permeability curves and cleat porosity from simulated production data in this study. Comparison of derived parameters from simulated production data with input parameters helps to assess the effect of cross-formational flow on PDA

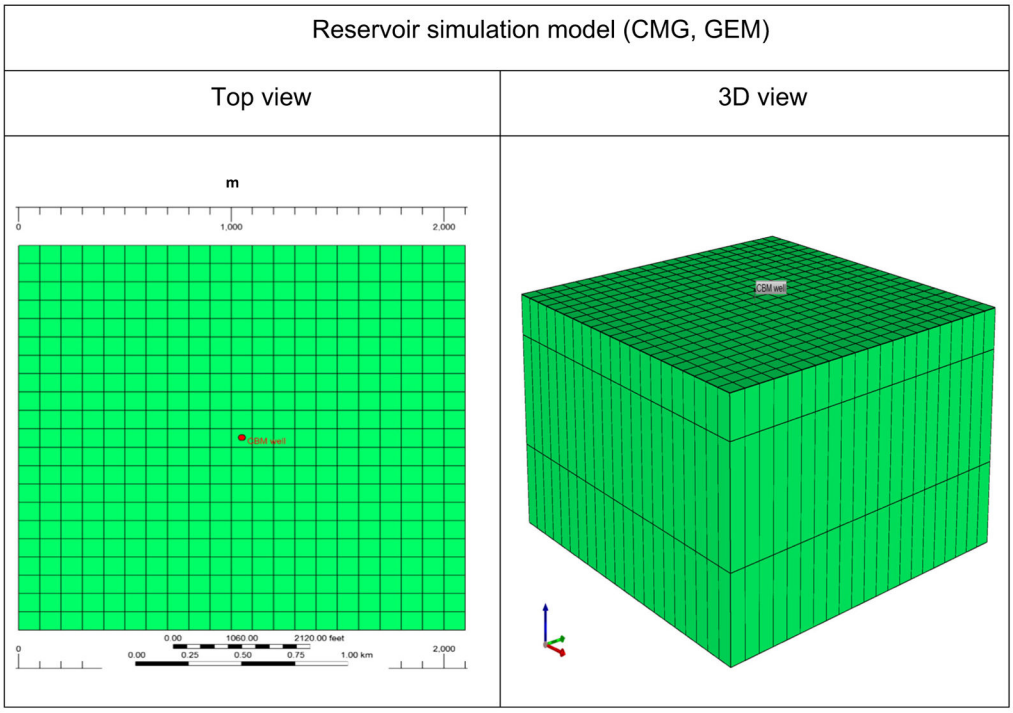

Fig. 3.

Reservoir simulation model constructed by CMG reservoir simulator. This single-well model is used to investigate the effect of water flow from the overlying formation into the coal section on production performance of the well

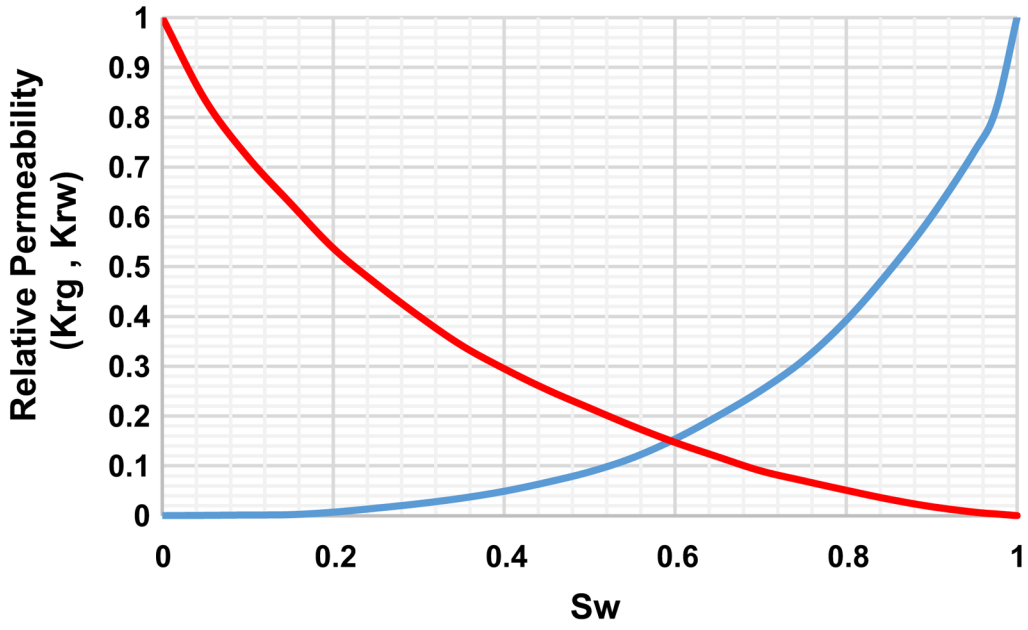

Fig. 4.
Input relative permeability curves for coalbed and the overlying formation (Gash 1991)

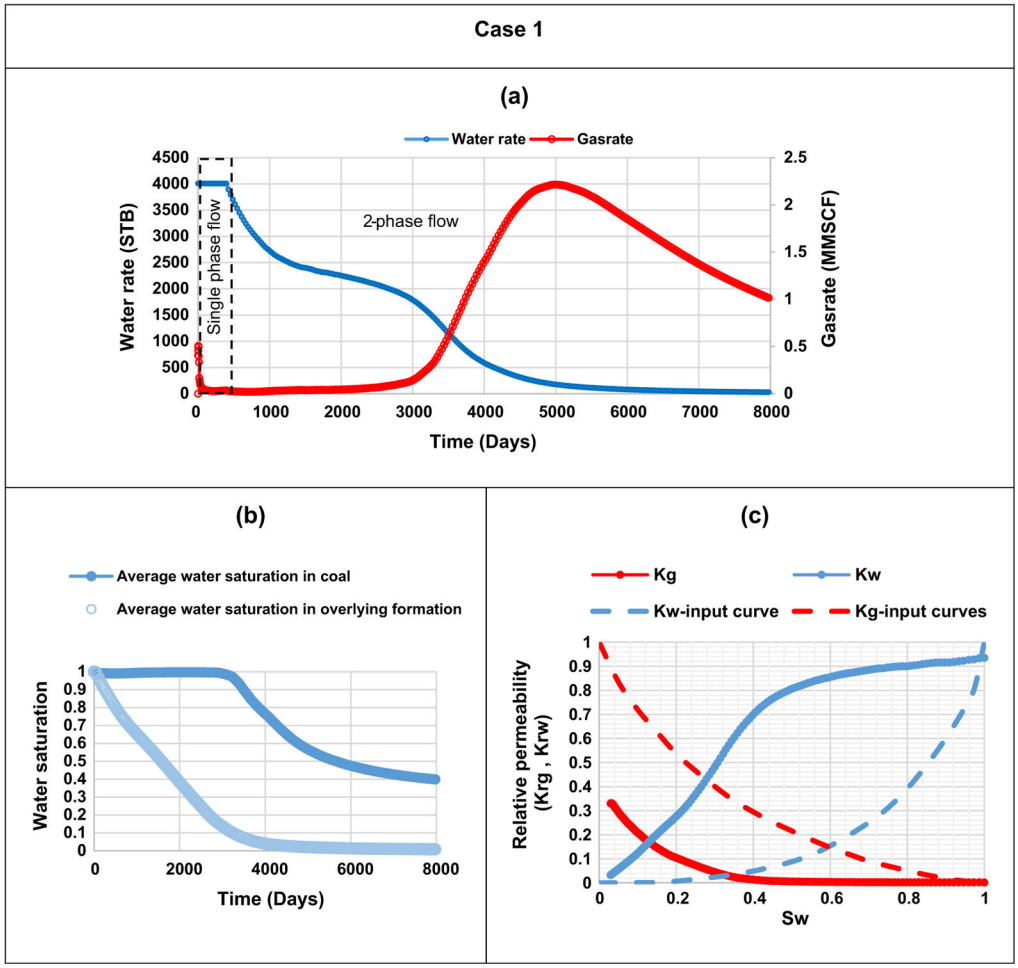

Fig. 5.

Simulation results demonstrated for case 1: **a** gas and water production profiles generated by reservoir simulation, **b** average water saturation in coalbed remains close to 1 for an extended period of time while water saturation drops in the overlying formation, **c** derived gas and water relative permeability curves from production data when cross-formational flow is overlooked. Derived curves are compared with the input curves

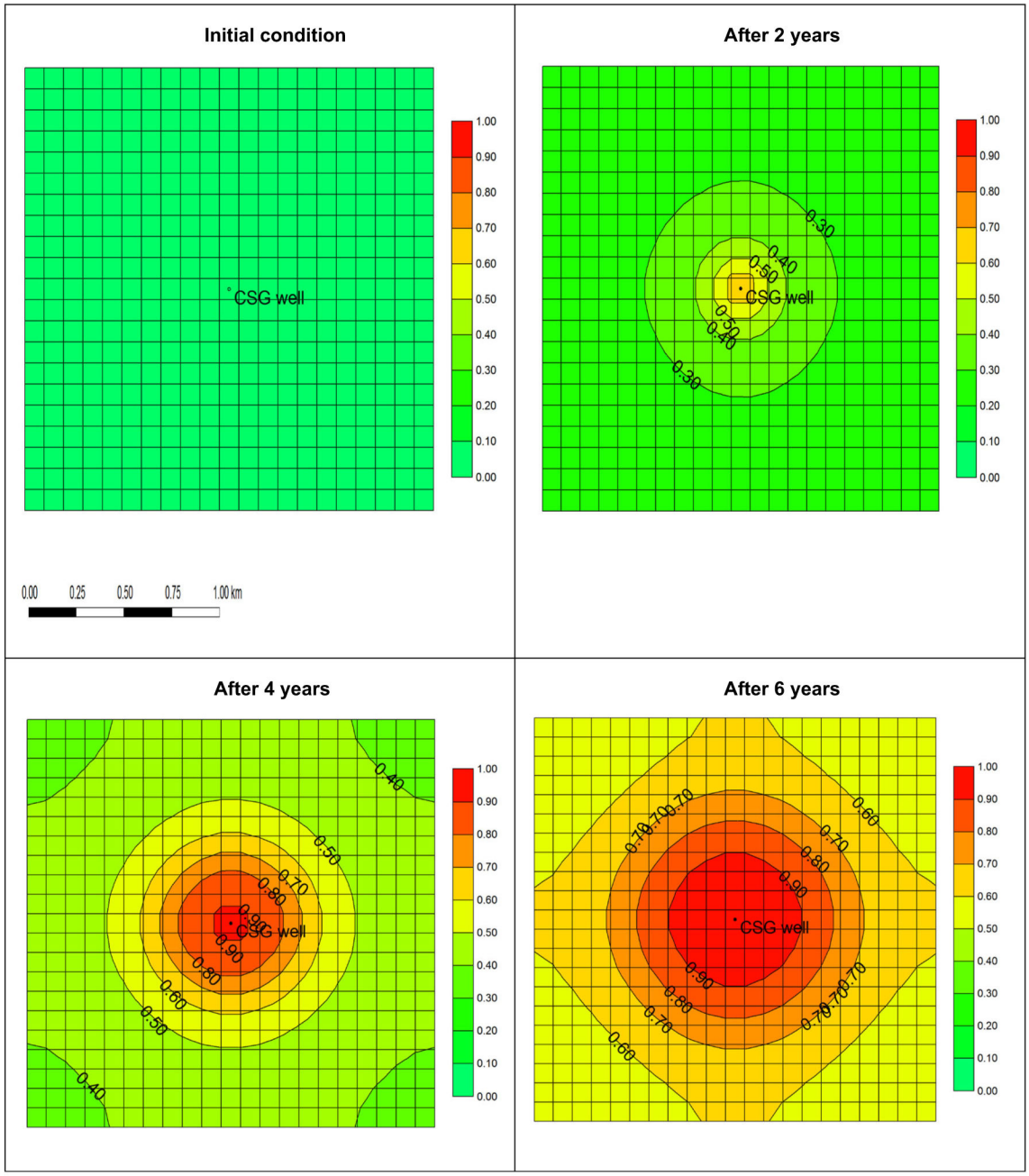

Fig. 6.

Evolution of gas saturation in the overlying formation. During production, desorbed gas from the coal layer migrates upward to the top formation and gas saturation increases

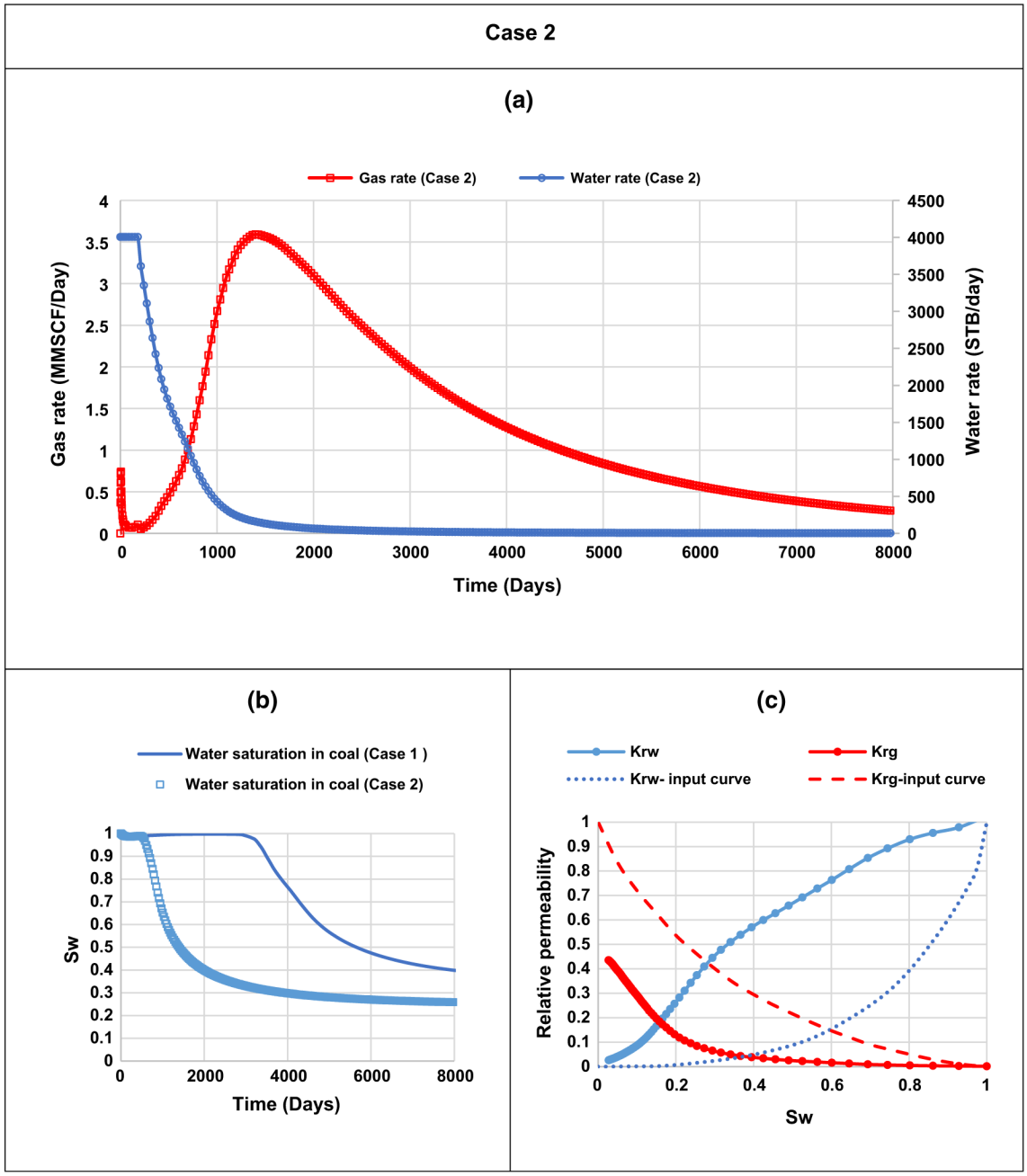

Fig. 7.

a Production history for the second case. **b** Comparison of water saturation in coal for case 1 and case 2. **c** Comparison of input relative permeability curves with the ones derived from production data

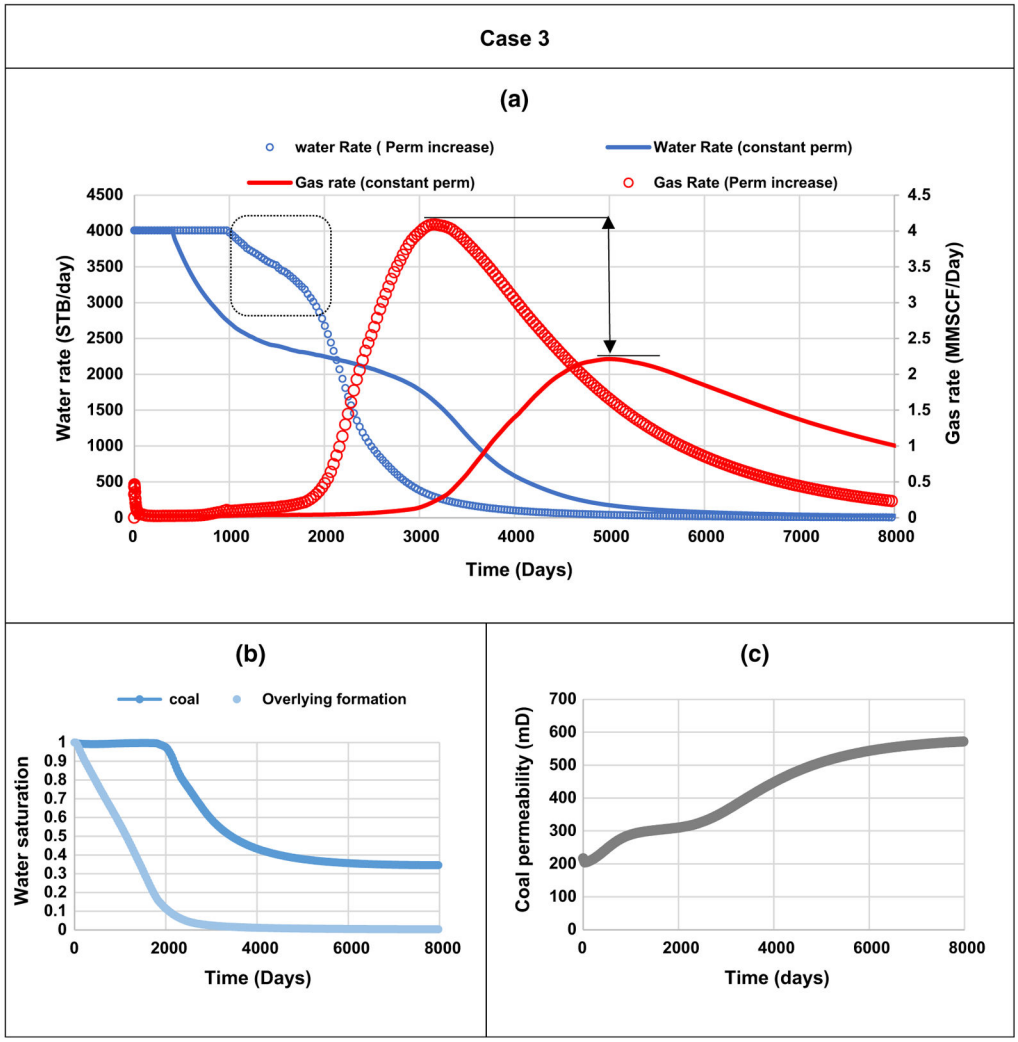

Fig. 8.

Simulation results for case 3, **a** comparison of gas and water production rates for case 3 with the first case in which permeability is constant during production. When permeability increases, time of peak gas production is brought forward and peak gas rate is almost double **b** average water saturation in coalbed and overlying formation **c** permeability varies during production and is calculated by the Palmer–Mansoori model

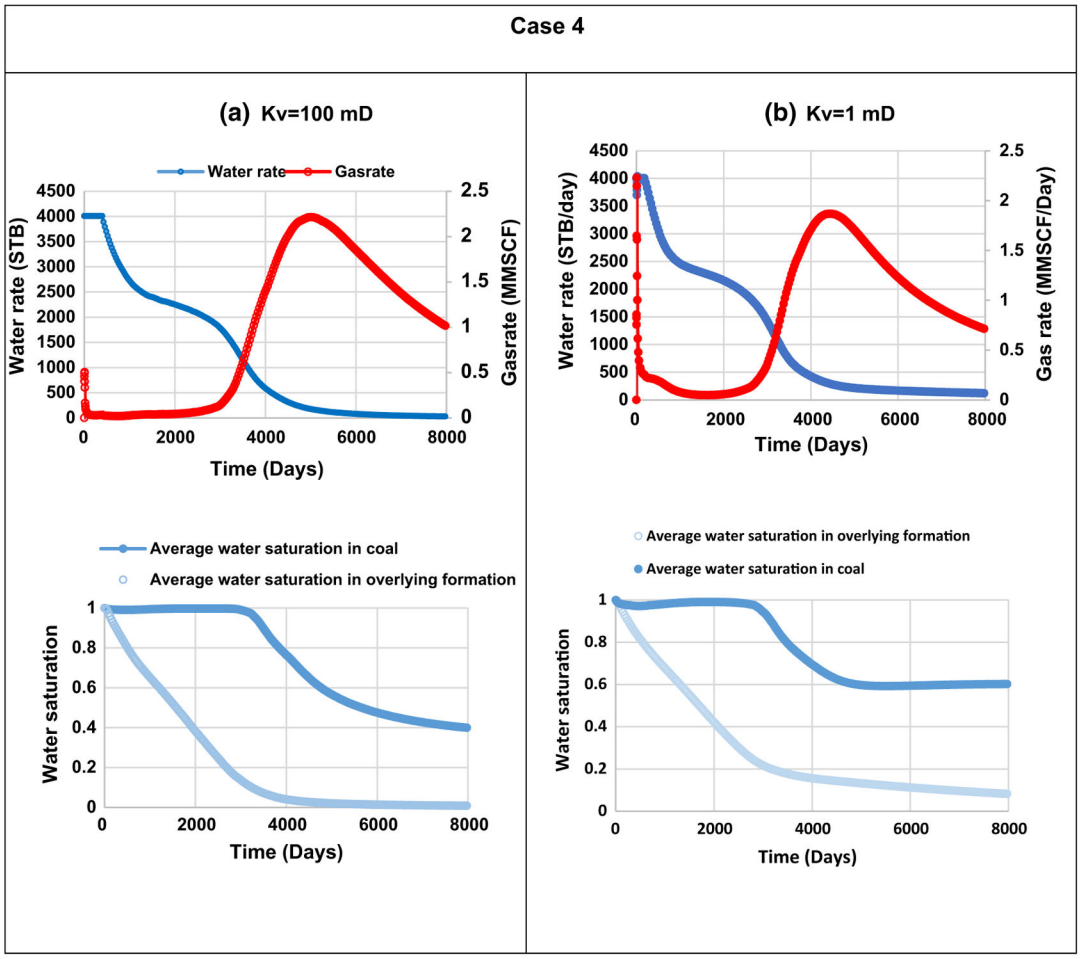

Fig. 9.

Sensitivity of gas and water production profiles to vertical conductivity between the overlying formation and the coalbed, **a** gas and water production history when vertical permeability in the overlying formation is 100 mD (case 1), **b** production history when vertical permeability of the overlying formation is set to 1 mD

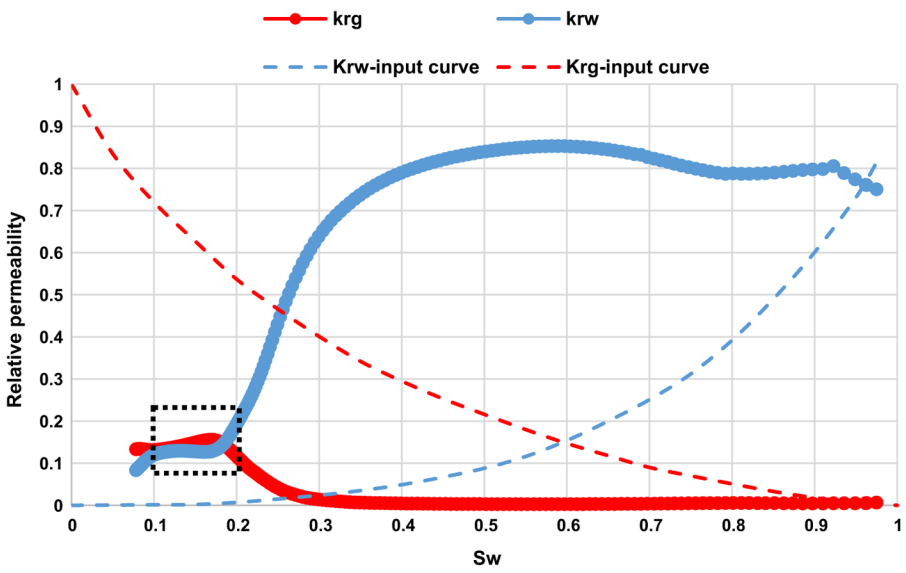

Fig. 10.

Gas and water relative permeability curves, derived from production data for case 4, are compared with input curves used in the simulation model. Water saturation stabilization/ rebound in coal at late time results in relative permeability curves to have approximately flat shapes when water saturation changes from 0.2 to 0.1 (see the *dashed box*)

Table 1

Reservoir parameters used as inputs in the reservoir simulation model

Properties	Value
Thickness of the overlying formation (ft)	11.15
Porosity of the overlying formation (%)	9.16 and 2
Vertical permeability of the overlying formation (mD)	100
Coal thickness (ft)	31
Coalbed depth (ft)	2194
Horizontal permeability in coal (mD)	217
Vertical permeability in coal (mD)	21.7
Drainage area (acres)	1090
Coal specific gravity	1.435
Cleat porosity (%)	0.2
Langmuir volume (SCF/ton)	664
Langmuir pressure (psia)	438
Initial reservoir pressure (psia)	942
Critical desorption pressure (psia)	837
Wellbore radius (ft)	0.65
Well skin factor	0

Table 2

Cleat porosities used in production history matching techniques in various basins worldwide

Author and Year	Study area	Cleat porosity used in matching techniques (%)
McKee and Bumb (1987)	San Juan Basin, USA	4
Zuber et al. (1987)	Black Warrior Basin, USA	2
Sawyer et al. (1990)	Black Warrior Basin, USA	3
Young et al. (1991)	Cedar Hill Field, Northern San Juan Basin, USA	0.25–0.8
Ried et al. (1992)	Powder River Basin, USA	4
Shi and Durucan (2004)	San Juan Basin, USA	0.2
Aminian et al. (2004)	Appalachian Basin, USA	2–3.5
Wong et al. (2007)	South Qinshui Basin, China	0.8
Clarkson et al. (2007)	Horse shoe canyon, Canada	0.1
Shi and Durucan (2010)	San Juan Basin, USA	0.035–0.11
Moore et al. (2011)	San Juan basin, USA	0.055–0.17
Clarkson et al. (2011)	San Juan Basin, USA	0.16
Karacan (2013)	Black Warrior Basin, USA	0.27–5.65
Mazumder et al. (2013)	Surat Basin, Australia	0.6–2
Karacan et al. (2014)	Illinois Basin, USA	1–6
Yarmohammadtooski et al. (2016)	Bowen Basin, Australia	5

Table 3

Parameters used in the Palmer–Mansoori model

Parameter	Value
Poisson ratio	0.39
Young modulus of elasticity (psia)	445,000
Strain at infinite pressure	0.01266
Langmuir pressure (psia)	438
Palmer–Mansoori exponent	3
Cleat compressibility ($psia^{-1}$)	0.000146
Cleat porosity (%)	0.2